ISSN 1560-8034, 1605-6582 (On-line), SPQEO, 2019. V. 22, N 2. P. 206-214.

Hetero- and low-dimensional structures

Formation of nanocrystals and their properties during tin induced and laser light stimulated crystallization of amorphous silicon

V.B. Neimash[1], A.S. Nikolenko[2], V.V. Strelchuk[2], P.Ye. Shepeliavyi[2], P.M. Litvinchuk[1], V.V. Melnyk[1], I.V. Olhovik[1]

[1]*Institute of Physics, NAS of Ukraine*
46, prospect Nauky, 03680 Kyiv, Ukraine
[2]*V. Lashkaryov Institute of Semiconductor Physics, NAS of Ukraine*
41, prospect Nauky, 03680 Kyiv, Ukraine
E-mail: neimash@gmail.com

Abstract. The effect of laser light intensity and temperature on the induced tin crystallization of amorphous silicon has been investigated using the methods of Raman scattering and optical microscopy. The existence of non-thermal mechanisms of the laser light influence on formation of silicon nanocrystals and their Raman spectra has been experimentally demonstrated. Photoionization of silicon and electron-phonon interaction are considered as possible reasons for the detected effects. The prospects of their application in new technologies providing production of nano-silicon films for solar cells have been discussed.

Keywords: amorphous silicon, crystallization, tin, qq photoionization, electron-phonon interaction, solar cells.

https://doi.org/10.15407/spqeo22.02.206
PACS 63.22.Kn, 64.70.Nd, 64.70.dg

Manuscript received 26.03.19; revised version received 24.04.19; accepted for publication 19.06.19; published online 27.06.19.

1. Introduction

The film composite "Si nanocrystals in the amorphous Si matrix" (nc-Si) is a promising material for the next generation of solar cells (SC) with quantum dots [1]. It has a unique set of physical properties: the direct-gap mechanism of light absorption, band gap width dependence on the size of nanocrystals, resistance to the Stebler–Wronsky effect, the ability to grow on flexible substrates.

Using nano-silicon to create isomorphous hetero-structures of the cascade type [2, 3] can substantially increase the efficiency and reduce the cost of SC due to the advantages of thin-film and roll technologies [4, 5]. Among the main problems hampering the practical realization of the advantages of nc-Si is the lack to develop technology for controlling the size and concentration of Si nanocrystals at economically feasible rates of film formation. Therefore, despite the large number of existing nc-Si manufacturing technologies, much attention is paid to improve them and find the new ones (for example [6-12]).

One of the promising ways in this direction is to use the phenomenon of metal induced crystallization (MIC) of amorphous silicon [13-17]. In particular, at the beginning of the latter decade, the possibility to form Si nanocrystals with dimensions close to 2…5 nm and the fraction of phase volume up to 80% in the matrix of amorphous Si was demonstrated using low temperature crystallization of amorphous Si stimulated with tin [18-20]. The indicated experimental results were interpreted using the new mechanism of MIC proposed in [20, 21] and theoretically grounded in [22]. It differs significantly from those known for other metals [13, 15-17]. According to this mechanism, silicon nanocrystals are formed as a result of cyclic repetition of the processes of formation and decomposition of a supersaturated silicon solution in tin in a narrow layer of eutectics on the interface of amorphous silicon and metal tin. It turned out that this process may be launched using laser light at relatively high intensity ($I \sim 10^5$ W/cm^2), which is used to excite the Raman light scattering. In [23], during measurements of Raman spectra, formation of silicon nanocrystals of one nanometer size in the layer of amorphous silicon in a two-layer silicon-tin film was observed. According to the performed measurements and estimates, as a result of absorption of the energy of laser excitation of the Raman scattering, the temperature of the film under the beam can reach 700 °C. This initiates MIC processes that convert Si from amorphous to a nano-

crystalline state. The analysis of the Raman spectra recorded at this moment makes it possible to measure not only the temperature but also the size and concentration of nanocrystals. This makes it possible to control formation of nanocrystals by changing the intensity and exposure time of the laser beam. The authors of [23] noticed that the growth and accumulation of silicon nanocrystals under the laser beam are faster than when it's heated to the same temperature in the dark.

On this basis, they assume that photoionization of silicon somehow contributes to the processes of MIC. In favor of this assumption, the results of recent work [24] show that stimulating effects of short (10 ns) but powerful (up to ~10^8 W/cm^2) single laser pulses on MIC in the a – (Si/Sn) system were also observed.

In this paper, we are going to show that the processes of tin induced crystallization (TIC) of amorphous silicon can be accelerated by laser light with no effect of the temperature. In addition, we demonstrate that the Raman spectrum of newly formed silicon nanocrystals is sensitive to the intensity of the laser light even at a stable temperature, in contrast to the spectrum of monocrystalline silicon.

2. Experimental

Objects of our researches were planar bilayer structures "amorphous silicon on metal tin" on the substrates of borosilicate glass (BSG) or monocrystalline silicon of the brand CEF-4,5. These were made by successive deposition of tin (99.92%) and silicon (99.999%) thermally evaporated in vacuum from tantalum evaporators, heated by electric current. The deposition took place on glass or silicon substrates 1 and 0.3 mm thick, respectively, at the temperature close to 150 °C in the sequence: a layer of tin on the substrate, then a layer of silicon over the layer of tin. The thickness of the layers was discretely varying within the range from 50 up to 200 nm with the step 50 nm. Both deposition was carried out in one vacuum chamber without depressurization at the residual pressure of 10^{-3} Pa by successive use of two different evaporators.

Behavior of the Raman spectrum of the surface layer of the structures described at various substrate temperatures and at different intensities of the exciting light was investigated.

Raman spectra were measured in the inverse scattering geometry of Horiba Jobin Yvon T64000 spectrometer with Olympus BX41 confocal microscope and thermoelectrically cooled CCD detector. Spectral resolution was 0.15 cm^{-1}. To excite Raman spectra, the Ar-Kr line of the laser with the wavelength λ = 488.0 nm was used. Exciting radiation was focused on the surface of the tested sample by using the Olympus 50× lens (*NA* = 0.5) in an area of 1 μm with a maximum power close to 10 mW (100%) or that weakened with neutral filters down to 50%, 25%, 10%, 1%. In this case, the power density of the excitation radiation per sample varied within the limits from 10^4 to 10^6 W/cm^2. For temperature-dependent Raman measurements with

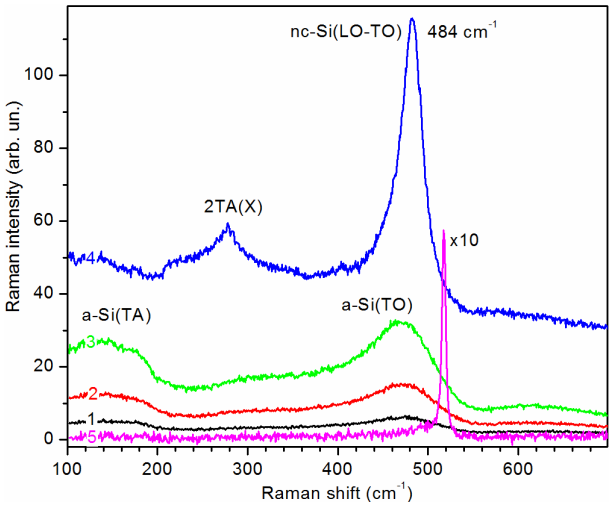

Fig. 1. Raman spectra of the structure BSG \ Sn (100 nm) \ a-Si (100 nm). *1* – *P* = 1 mW, *2* – 2.5, *3* – 5.0, *4* – 10, *5* – 0.1. ν_{max} = = 484 cm^{-1}.

controlled thermal heating, the samples were placed in a thermoelectric cell Linkam THMS600. The temperature in it was varied discretely within the range 20 to 550 °C with an accuracy ±0.1 °C . Raman spectra were measured within the range of 100 to 850 cm^{-1}. The scanning time (which is the time of the exciting laser beam action on the sample) was 50 or 100 s.

The surface of the samples was controlled visually using an optical microscope using the 50-fold lens and with a digital camera in the laser beam area and around it.

3. Results and discussion

Fig. 1 shows the Raman spectra of the BSG \ Sn (100 nm) \ a-Si structure (100 nm) on the glass substrate, written with successively increased laser excitation power (50-s scan time).

It is seen that only at the maximum power (10 mW) a crystalline phase of silicon appears at a maximum of 482 cm^{-1}, which is preserved and under further decrease of the light power to the minimum (0.1 mW), moving to the maximum position at 517 cm^{-1}. The analysis of this spectrum using the method [25, 26] shows formation of silicon nanocrystals with a dominant size *R* = 5 nm, which occupy more than XC = 58% of the material in the spot of the Raman spectrum measuring.

In the samples on a BSG \ Sn (150 nm) \ a-Si (50 nm) glass substrate, the heat transfer conditions from the laser action area in the silicon layer are a little bit better due to greater thickness of the metal layer and less silicon. Obviously, because of it, crystallization in this case is slower, although only with a laser power of 10 mW. Raman spectra recorded on a sample of this structure are shown in Fig. 2. It can be seen that the gradual increase in power up to 9 mW inclusively does not cause any signs of a crystalline component in the Raman spectrum.

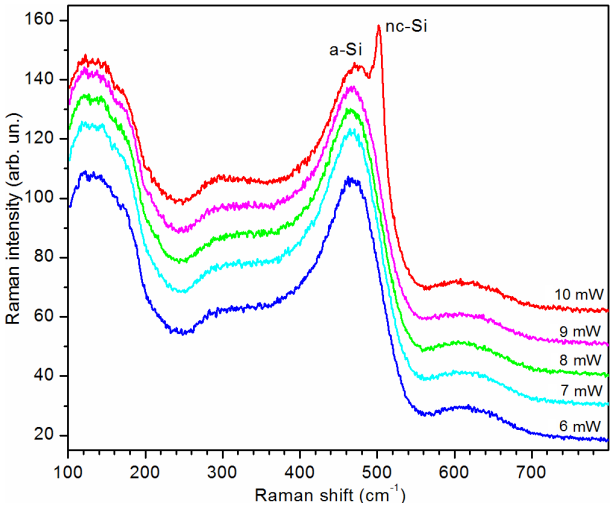

Fig. 2. Raman spectra of the BSG \ Sn (150 nm) \ a-Si structure (50 nm) at different laser excitation power capacities.

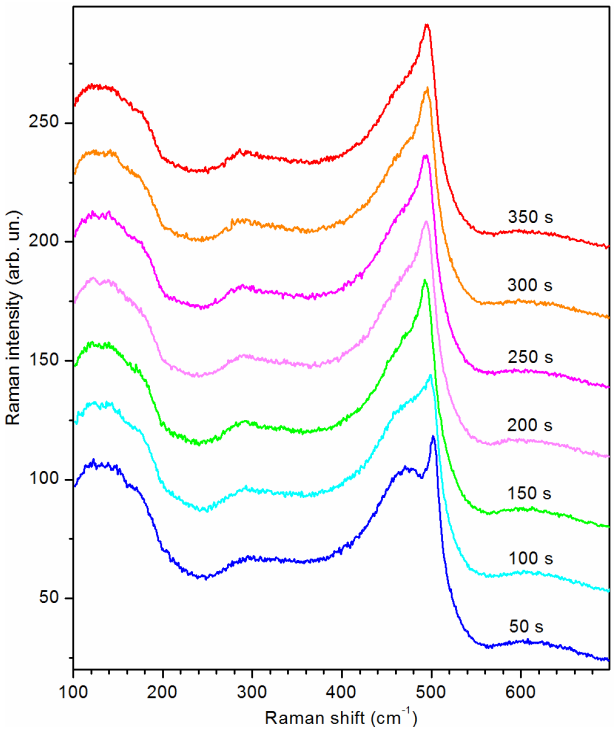

Fig. 3. Effect of duration of laser light action with the power of 10 mW on the Raman spectrum shape.

However, the further increase in power up to 10 mW results in the jump-like appearance of a crystalline component, which corresponds to nanocrystals of the size $R = 4.5$ nm and the volume fraction XC = 34%.

It is typical that repeated scanning the spectrum of the same place of the sample (i.e., accumulation of the laser radiation time up to 300 s) at $P = 10$ mW shows a gradual increase in crystallite sizes up to $R = 5$ nm and their volume fraction to XC = 47%. This is illustrated in Fig. 3 that shows an increase in the ratio of the amplitudes of the crystalline and amorphous components of the main Raman band with the laser action time from 50 to 350 s.

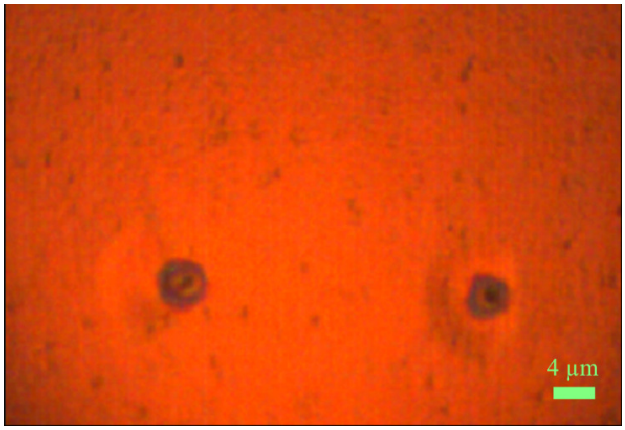

Fig. 4. Optical microphotography of the surface of the tested sample. Two concentric spots are typical traces of a laser beam with a power of 10 mW.

Thresholds of the dependence of TIC on the power of laser light were observed in [24]. The authors suggested that the threshold is due to the achievement of a tin melting temperature (230 °C), which in fact coincides with the point of the eutectic of the Si-Sn pair. In fact, according to [20-22] tin induces crystallization of amorphous silicon, passing through the state of liquid eutectic. Indeed, after crystallization on the surface of the samples, the traces of laser action remain visible in the optical microscope, as shown in Fig. 4. They are in the form of concentric circles, which differ significantly in contrast. We can assume that a black spot with the diameter of about 1 μm in the center is due to an amorphous-crystalline Si composite, which Raman spectrum we observe; light ring around the central spot – the exit to the surface of molten tin; broad dark circle of quasi-dendrite form – the zone of lateral crystallization from the tin ring. Finally, the outer light circle is similar to the depression – the region of deformation of the surface of the film of amorphous silicon as a result of a decrease in its thickness as a result of transverse crystallization from the bottom of the molten tin of the lower layer.

It should be noted that the different sizes and shapes of the spots of at least three levels of contrast appear on the surface of similar samples and after annealing in the dark in the oven at 300 °C for 30 min. But their Raman spectra contain only bands of amorphous silicon and tin oxide without any signs of crystalline silicon. That is, the laser light with the power close to 10 W/μm^2 for 1 to 6 min can translate about half the silicon into a layered structure of a-Si\Sn from amorphous to the crystalline state, which requires at least an order of magnitude longer in terms of heat treatment in the dark.

There may be at least two reasons for this: 1) the temperature of the laser beam is much higher than 300 °C; 2) there is a non-thermal mechanism of light stimulation of amorphous silicon during TIC.

To check up these assumptions, the following experiments were carried out. In order to reduce the local warming of the sample at the point of the laser beam

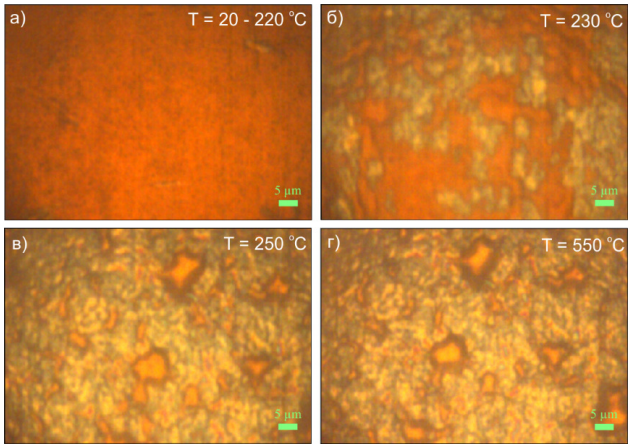

Fig. 5. View of the sample surface after heating up to 20…220 °C (a), 230 (b), 250 (c), and 550 (d).

focus, we increased the heat dissipation, replacing the substrate material with a more heat conductive material. In completely similar conditions, a layered structure of amorphous silicon and metal tin with a similar thickness ratio was made, but on a substrate of monocrystalline silicon with the thickness 300 μm with the specific resistivity 4.5 Ohm·cm, which thermal conductivity is much higher than that of boron-silicate glass. The crystal silicon band in the Raman spectrum of this substrate at room temperature changes its position no more than 0.2 cm^{-1} when the Raman excitation power changes from 0.1 to 10 mW. That is, at the point of focusing laser excitation, even at the maximum power, the substrate temperature rises by no more than 10 °C [27, 28]. The influence of the substrate temperature and laser radiation

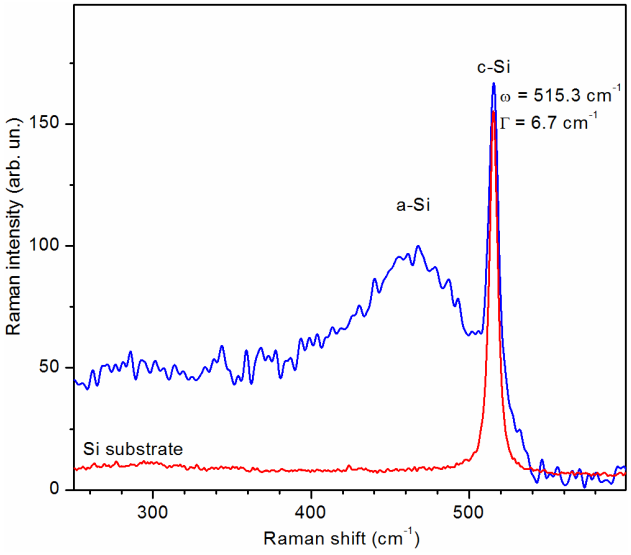

Fig. 6. Raman spectrum of the structure c-Si \ Sn (150 nm) \ a-Si (50 nm). The Raman spectrum of monocrystalline silicon substrate (red curve) is given for comparison. T = 230 °C, P = 2.5 mW.

power on the Raman spectrum of the c-Si \ Sn (150 nm) \ a-Si structure (50 nm) was investigated within the temperature range 20…550 °C by using the Linkam THMS600 thermoelectric cell that automatically supports the set temperature values with the accuracy ∓0.1 °C .

No effect of laser light in the whole range of powers from 0.1 mW to 10 mW on the TIC of amorphous silicon in this structure on the silicon substrate is observed not only at room temperature of the sample, but also when it is heated in the furnace up to T = 220 °C inclusively. Only at 230 °C and above, when there were signs of melting of the tin layer, laser irradiation of maximum power causes rapid crystallization of amorphous silicon, like to the structures on the glass substrate. Fig. 5 shows how the surface of the tested sample changes in the optical microscope during heating in the thermoelectric cell.

After 2-3 min passage over the temperature range 230…240 °C, a green-yellow spot appears on the initially homogeneous surface of the purple color (Figs. 5a and 5b). Obviously, it is caused by the transition of tin layer into the liquid state, which is accompanied by formation of microscopic tin droplets [20, 23] in these thin layers and by the rupture of an outer three-fold thinner film of amorphous silicon. For 7-8 minutes, when the temperature stabilizes at 250 °C, the area of purple and yellow-green regions is approximately comparable, like to that in Fig. 5c. For 2-3 min the growth of yellow-green areas is gradually ceasing. The further increase in temperature up to 550 °C leads only to a certain increase of the dark halo around the yellow spots due to their decrease (Fig. 5d).

The Raman spectrum in the regions of the purple color corresponds to the spectrum of amorphous silicon. In the spectrum of yellow-green areas there is a crystalline component. The position of its phonon band at T = 230 °C is at the frequency 515.3 cm^{-1} (Fig. 6), and its amplitude increases almost twice in 10 min, and then does not change over time.

Simultaneously, the peak position is shifted downward in frequency with increasing the temperature with a tempo of 2 cm^{-1} at 100 °C, and the band itself in its position and shape coincides with the spectrum of the substrate of monocrystalline silicon (has a symmetrical contour with the half-width of 6.7 cm^{-1} at 230 °C), which in the normalized form is shown in Fig. 6 for comparison. These facts uniquely identify this band with Raman scattering of a monocrystalline substrate. Apparently, its observation was made possible by the intervals between microscopic droplets of tin, which are formed by the action of forces of surface tension in a layer of molten tin that has poor adhesion to the silicon substrate. This formation of tin micro-droplets under the similar conditions was observed in [20, 23]. The gradual exit to the inpatient of the intensity of the band 515.3 cm^{-1} over time in this case is explained by completion of the process of formation of tin droplets and the corresponding increase in the intervals between them, through which the light can pass into a silicon substrate heated to 250 °C.

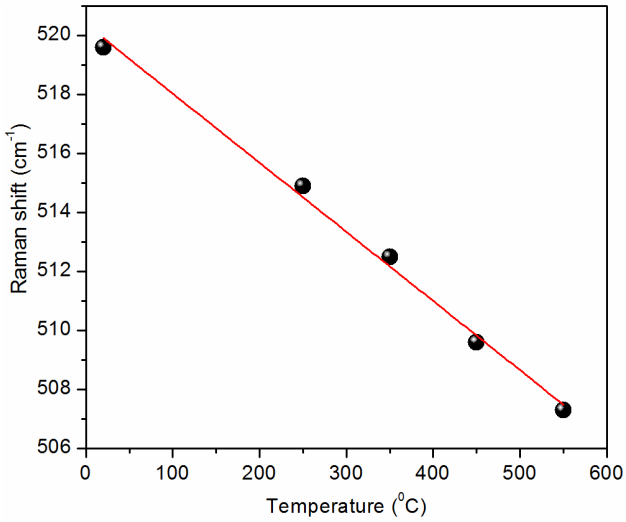

Fig. 7. Temperature dependence of the frequency position inherent to the phonon band of the silicon crystalline phase that appears in the structure of c-Si \ Sn (150 nm) \ a-Si (50 nm) at T = 230 °C, P = 2.5 mW. Points – experimental data, line – approximation.

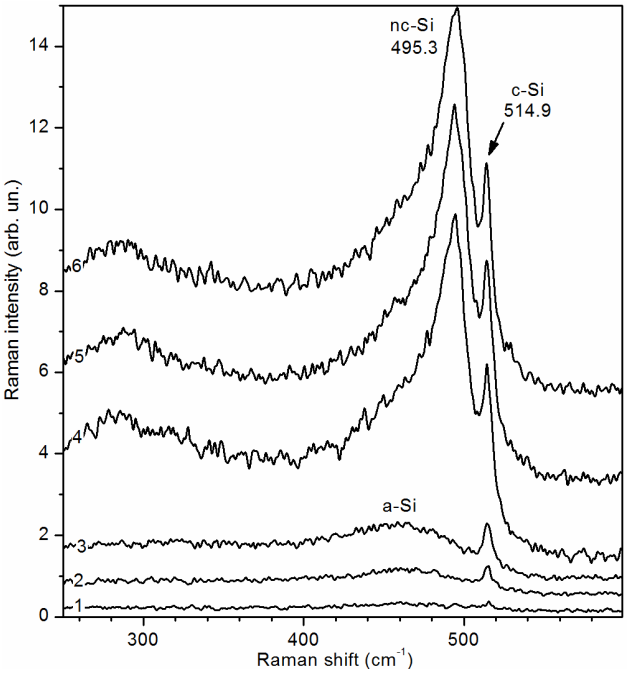

Fig. 8. Raman spectra of c-Si \ Sn (150 nm) \ a-Si structure (50 nm) heated to T = 250 °C with increasing the laser excitation power P, mW: 1 (*1*), 2.5 (*2*), 5 (*3*), 10 (*4*, *5*, *6*).

The further increase in temperature from 250 to 550 °C does not affect the amplitude of the band, but shifts its peak downward in frequency. After cooling the sample to room temperature, its position is about 520 cm^{-1}. Fig. 7 shows the dependence of the frequency position of the band peak on the sample temperature. It is seen that it has a linear character and fully corresponds to the temperature dependence of the position inherent to the phonon band of monocrystalline silicon [27, 28].

We used this band as a reference object for further investigation of the effect of laser excitation power on the Raman spectrum of this structure. Fig. 8 shows the Raman spectra obtained with the sample heated to 250 °C with increasing power P from 1 to 10 mW. It is seen that, at the powers 1, 2.5 and 5 mW in the spectra, there is only one band of the crystalline phase – the band of monocrystalline substrate at 514.9 cm^{-1}. At P = = 10 mW, like to the similar structure on the glass substrate, a band of a nanocrystalline component appears at 496 cm^{-1} with the half-width 24 cm^{-1}. In addition, its amplitude immediately almost triplicates the amplitude of the phonon band of the substrate, whose frequency position remains unchanged at 514.9 cm^{-1}. It is indicative of no influence of laser radiation on the temperature of the investigated sample area. That is, there is a non-thermal mechanism of laser-assisted TIC.

Two additional scans of the spectrum (5 and 6 in Fig. 8) at P = 10 mW (that is, the shutter speed at 250 °C under laser light additionally 100 s) practically does not affect either the amplitude or the frequency position of the phonon band of nanocrystals. It means that formation of nanocrystals under these experimental conditions takes place very quickly and ends with less than 1\2 scan times of the spectrum – 25 s.

A similar nature of the effect of laser irradiation intensity on TIC is observed at all temperatures above 230 °C, that is, above the melting point of tin. It means that the liquid state of tin and the density of light power of at least 10 mW/μm^2 alone are necessary but not sufficient conditions for the laser acceleration of the effect of TIC in the system a-Si\Sn. Only their simultaneous combination causes the effect of accelerating crystallization of amorphous silicon by at least one order of magnitude as compared to heat treatment in the dark.

This result is fully consistent with the data of our previous works [23, 24], which raises the question of the non-thermal nature of the stimulating effect of light on MIC of amorphous silicon.

The presence of the Raman band inherent to the monocrystalline substrate can illustrate the dependence of the Raman scattering by silicon nanocrystals on the intensity of excitation by laser light at a stable temperature of the sample. Fig. 9 shows behavior of the Raman spectra of the structure on a silicon substrate, similar to the previous one, but after crystallization at a decrease in the power of laser radiation from 10 to 1 mW. It is seen how the peak of nanocrystals shifts from 500.5 cm^{-1} at P = 10 mW to 509.5 cm^{-1} at P = 5 mW, to 512 cm^{-1} at P = 2.5 mW and at the end to 513 cm^{-1} at P = = 1 mW, covering the peak of the monocrystalline substrate at 515 cm^{-1}, which, by its frequency position (as seen from Fig. 8), does not react to the change in power within this range.

A similar effect of the influence of the laser light power of Raman excitation on the frequency position of the nanocrystalline silicon band is observed at all temperatures within the considered range. In particular, in Fig. 10 it is shown how, at room temperature, the band

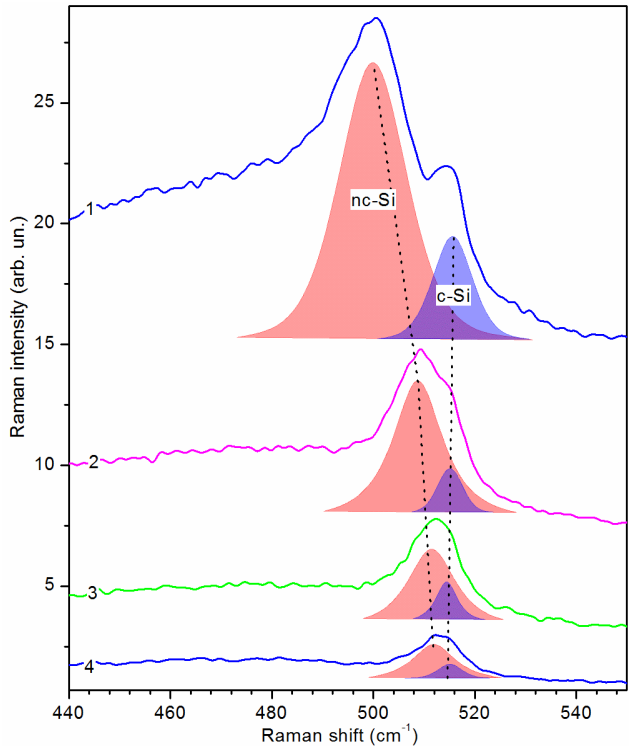

Fig. 9. Raman spectra of the structure c-Si \ Sn (150 nm) \ a-Si (50 nm) heated to T = 250 °C, with decreasing the power P of the laser beam: 10 mW (*1*), 5 (*2*), 2.5 (*3*), 1 (*4*).

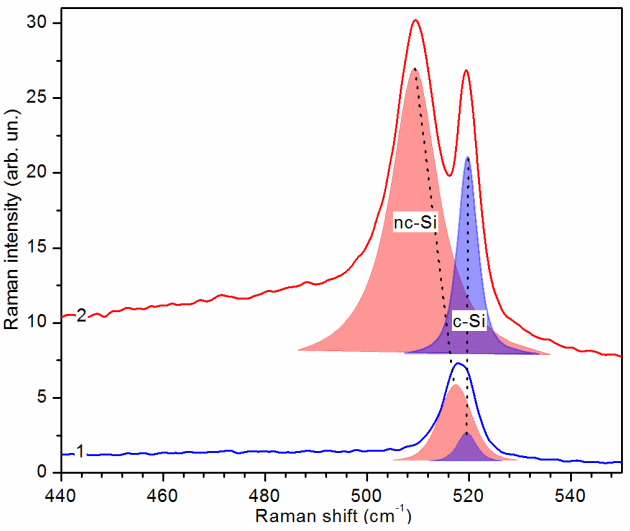

Fig. 10. Raman spectra of the structure c-Si \ Sn (150 nm) \ a-Si (50 nm) laser-modified at T = 250 °C, P = 10 mW, measured at 230 °C and laser excitation powers P = 2.5 mW (*1*), 10 mW (*2*).

of the Si crystalline phase, formed at T = 250 °C, splits into two components with increasing the power of laser beam providing Raman excitation. It can be seen that the only band at P = 2.5 mW of the Si crystalline phase at about 518 cm^{-1}, splits at P = 10 mW by the substrate band 520 cm^{-1} and a band of 508 cm^{-1} nanocrystals.

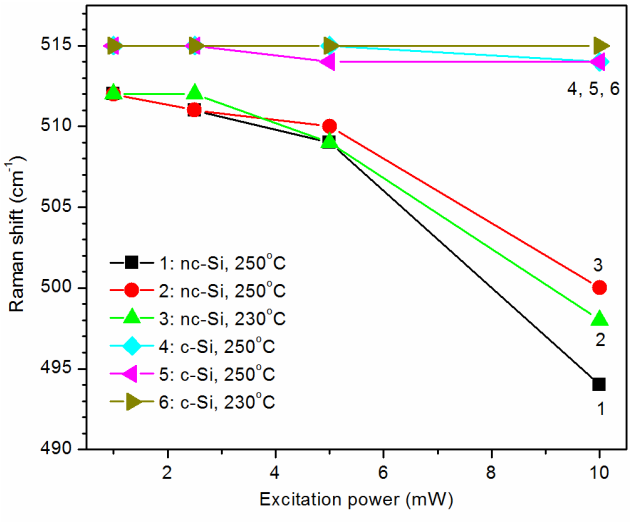

Fig. 11. Dependences of the frequency position of the Raman bands of nanocrystallites (*1*, *2*, *3*) and monocrystalline substrate (*4*, *5*, *6*) at the temperatures of 250 °C (*1*, *2*, *4*, *5*) and 230 °C (*3*, *6*) on the laser excitation power.

The results of the analysis of Raman spectra measured at different places of the c-Si \ Sn (150 nm) \ a-Si structure (50 nm) at different laser excitation intensities and at temperatures of 230 °C and 250 °C are summarized in Fig. 11. In particular, the dependence of the frequency position for phonon peaks of the nanocrystalline phase (*1*, *2*, *3*) and monocrystalline substrate (*4*, *5*, *6*) on the intensity of laser excitation is shown. It is seen that the position of the phonon peak inherent to the substrate does not depend on the intensity of laser excitation. At the same time, the peak of nanocrystalline silicon is substantially shifted to the low-frequency side, increasing the nonlinear displacement with increasing intensity of light.

So, the Raman spectrum of nanocrystalline silicon, unlike to the monocrystalline one, is sensitive to the intensity of exciting radiation. In addition, this sensitivity is not associated with temperature changes, but is caused by the optical component of the influence of laser light. The above result is consistent with the data of works [29, 30], where an unusually strong “red shift” and the extension of the phonon band of Si nanocrystals were observed due to the high intensity of laser excitation. This effect in [28] was explained by the combined action of the effects of laser heating the nanocrystallites and non-equilibrium population of phonons arising from the electron-phonon interaction of photoinduced charge carriers due to the high rate of generation of the latter at high excitation powers. The limited length of diffusion of photoexcited charge carriers, which in the system of silicon nanocrystallites can be of the order of only ~0.2 Å, and which is considerably less than the diameter of the focused Raman excitation beam of ~1 μm, results in a high rate of excitation of optical phonons that cannot decay too quickly. Under these conditions, in the measurement region, a non-thermal distribution of phonons is realized, which depends on the level of optical excitation.

The latter influences the Raman spectrum of nanocrystals in the form of a low-frequency shift of the phonon band of nanocrystals and the distorted ratio of the Stokes and anti-Stokes components of the spectrum. In contrast to [30], where weakly heat conductive porous films (porosity of 30-40%) of silicon nanocrystals with a silicon oxide shell were investigated, they were placed on weakly heat conductive glass substrates, and where the effect of laser heating the nanocrystallites could be substantial, in our case this heating is unlikely, since nanocrystals have a good thermal contact with metal tin, because they are formed as a result of the disintegration of a silicon solution in tin, and which well conducts heat to the silicon substrate. Consequently, the difference between our experiment is that its conditions allow us to isolate the effect of the optical component of the laser action from the thermal energy in its pure form.

It is possible that the above non-thermal component of the influence of laser light on TIC of amorphous silicon, also associated with non-equilibrium photoconductors of charge, is confirmed. For example, by facilitating the dissolution of amorphous silicon in tin due to the weakening of interatomic bonds, formation of holes in them and screening by electrons was created by photoionization. This result can be an important step in the development of manufacturing technology and quality control of nanocrystalline silicon for isomorphic solar cells of the cascade type.

4. Conclusions

1. For the first time, experimentally proved has been the existence of a non-thermal component of the stimulating effect of laser light on processes of tin-induced transformation of silicon from amorphous to nanocrystalline state.

2. The existence of a non-thermal mechanism of influence of light intensity on the Raman spectrum of silicon nanocrystals, which is absent in its monocrystalline state, has been experimentally demonstrated. This result demonstrates the benefit of the hypothesis proposed in the recent paper [30] to change the phonon spectrum of nc-Si as a result of electron-phonon interaction with photoinduced charge carriers.

References

1. Beard M.C., Luther J.M., and Nozik A.J. The promise and challenge of nanostructured solar cells. *Nat. Nano.* 2014. **9**, No 12. P. 951. https://doi.org/10.1038/nnano.2014.292.
2. Alferov Z.I., Andreev V.M., and Rumyantsev V.D. Solar photovoltaics: Trends and prospects. *Semiconductors.* 2004. **38**. P. 899. http://dx.doi.org/10.1134/1.1787110.
3. Yan B., Yue G., Xu X., Yang J., and Guha S. High efficiency amorphous and nanocryistalline sillicon solar cells. *phys. status solidi.* 2010. **207**. P. 671. http://dx.doi.org/10.1002/pssa.200982886.
4. Lewis N.S. Toward cost-effective solar energy use. *Science.* 2007. **315**. P. 798. https://doi.org/10.1126/science.1137014.
5. Søndergaard R., Hösel M., Angmo D., Larsen-Olsen T.T., and Krebs F.C. Roll-to-roll fabrication of polymer solar cells. *Mater. Today.* 2012. **15.** P. 36. https://doi.org/10.1016/S1369-7021(12)70019-6.
6. Birkholz M., Selle B., Conrad E., Lips K., and Fuhs W. Evolution of structure in thin microcrystalline silicon films grown by electron-cyclotron resonance chemical vapor deposition. *J. Appl. Phys.* 2000. **88**. P. 4376. https://doi.org/10.1063/1.1289783.
7. Rech B., Roschek T., Müller J., Wieder S., and Wagner H. Amorphous and microcrystalline silicon solar cells prepared at high deposition rates using RF (13.56 MHz) plasma excitation frequencies. *Sol. Energy Mater. Sol. Cells.* 2001. **66**. P. 267. https://doi.org/10.1016/S0927-0248(00)00183-5.
8. van Veen M.K., van der Werf C.H.M., and Schropp R.E.I. Tandem solar cells deposited using hot-wire chemical vapor deposition. *J. Non. Cryst. Solids.* 2004. **338-340**. P. 655. https://doi.org/10.1016/j.jnoncrysol.2004.03.071.
9. Mai Y., Klein S., Carius R., Stiebig H., Houben L., Geng X., and Finger F. Improvement of open circuit voltage in microcrystalline silicon solar cells using hot wire buffer layers. *J. Non. Cryst. Solids.* 2006. **352**. P. 1859. https://doi.org/10.1016/j.jnoncrysol.2005.11.116.
10. Li H., Franken R.H., Stolk R.L., van der Werf C.H.M., Rath J.K., and Schropp R.E.I. Controlling the quality of nanocrystalline silicon made by hot-wire chemical vapor deposition by using a reverse H2 profiling technique. *J. Non. Cryst. Solids.* 2008. **354**. P. 2087. https://doi.org/10.1016/j.jnoncrysol.2007.10.046.
11. Amrani R., Pichot F., Chahed L., and Cuminal Y. Amorphous-nanocrystalline transition in silicon thin films obtained by argon diluted silane PECVD, *Cryst. Struct. Theory Appl*. 2012. **1**. P. 57. http://dx.doi.org/10.4236/csta.2012.13011.
12. Fugallo G. and Mattoni A. Thermally induced recrystallization of textured hydrogenated nanocrystalline silicon. *Phys. Rev. B.* 2014. **89**. P. 045301. https://doi.org/10.1103/PhysRevB.89.045301.
13. Nast O. and Hartmann A.J. Influence of interface and Al structure on layer exchange during aluminum-induced crystallization of amorphous silicon. *J. Appl. Phys.* 2000. **88**. P. 716. https://doi.org/10.1063/1.373727.
14. Jeon M., Jeong C., Kamisako K. Tin induced crystallization of hydrogenated amorphous silicon thin films. *Mater. Sci. Technol.* 2010. **26**. P. 875. https: //doi.org/10.1179/026708309X12454008169500.
15. Mohiddon M.A. and Krishna M.G. Growth and optical properties of Sn–Si nanocomposite thin films. *J. Mater. Sci.* 2012. **47**. P. 6972. https://doi.org/10.1007/s10853-012-6647-0.

16. Van Gestel D., Gordon I., and Poortmans J. Aluminum-induced crystallization for thin-film polycrystalline silicon solar cells: Achievements and perspective. *Sol. Energy Mater. Sol. Cells.* 2013. **119**. P. 261. https://doi.org/10.1016/j.solmat.2013.08.014.
17. Ahamad Mohiddon Mahamad and Ghanashyam Krishna Mamidipudi. *Metal Induced Crystallization, Crystallization – Science and Technology*. M.R.B. Andreeta (Ed.). IntechOpen, 2012. DOI: 10.5772/50064.
18. Voitovych V.V., Neimash V.B., Krasko N.N., Kolosiuk A.G., Povarchuk V.Y., Rudenko R.M., Makara V.A., Petrunya R.V., Juhimchuk V.O., and Strelchuk V.V. The effect of Sn impurity on the optical and structural properties of thin silicon films. *Semiconductors.* 2011. **45**. P. 1281. https://doi.org/10.1134/S1063782611100253.
19. Neimash V.B., Poroshin V.M., Kabaldin A.M., Yukhymchuk V.O., Shepeliavyi P.E., Makara V.A., and Larkin S.Y. Microstructure of thin Si–Sn composite films. *Ukr. J. Phys.* 2013. **58**. P. 865. https://doi.org/10.15407/ujpe58.09.0865.
20. Neimash V., Poroshin V., Shepeliavyi P., Yukhymchuk V., Melnyk V., Kuzmich A., Makara V., and Goushcha A.O. Tin induced a-Si crystallization in thin films of Si-Sn alloys. *J. Appl. Phys*. 2013. **114**. P. 213104. https://doi.org/10.1063/1.4837661.
21. Neimash V.B., Goushcha A.O., Shepeliavyi P.E., V.O. Yukhymchuk, Dan'ko V.A., Melnyk V., and Kuzmich A. Mechanism of tin-induced crystallization in amorphous silicon. *Ukr. J. Phys*. 2014. **59**. P. 1168. https://doi.org/10.15407/ujpe59.12.1168.
22. Neimash V.B., Goushcha A.O., Shepeliavyi P.Y., Yuhymchuk V.O., Melnyk V.V., and Kuzmich A.G. Self-sustained cyclic tin induced crystallization of amorphous silicon. *Journal of Materials Research.* 2015. **30**, No 20. 3116. https://doi.org/10.1557/jmr.2015.251.
23. Neimash V., Shepeliavyi P., Dovbeshko G., Goushcha A., Isaiev M., Melnyk V., and Kuzmich A.G. Nanocrystals growth control during laser annealing of Sn:(α-Si) composites. *Journal of Nanomaterials.* 2016. **2016**. http://dx.doi.org/10.1155/2016/7920238.
24. Neimash V.B., Goushcha A.O., Fedorenko L.L., Shepeliavyi P.Ye., Strelchuk V.V., Nikolenko A.S., Isaiev M.V., and Kuzmich A.G. Role of laser power, wavelength, and pulse duration in laser assisted tin-induced crystallization of amorphous silicon. *Journal of Nanomaterials.* 2018. **2018**. https://doi.org/10.1155/2018/1243685.
25. Richter H., Wang Z.P., and Ley L. The one phonon Raman spectrum in microcrystalline silicon. *Solid State Communications.* 1981. **39**. P. 625. https://doi.org/10.1016/0038-1098(81)90337-9.
26. Campbell I.H. and Fauchet P.M. The effects of microcrystal size and shape on the one phonon Raman spectra of crystalline semiconductors. *Solid State Communications.* 1986. **58**. P. 739. https://doi.org/10.1016/0038-1098(86)90513-2.
27. Hart T.R., Aggarwal R.L., and Lax B. Temperature dependence of Raman scattering in silicon. *Phys. Rev. B.* 1970. **1**, No 2. P. 638. https://doi.org/10.1103/PhysRevB.1.638.
28. Tsu R. and Hernandez J.G. Temperature dependence of silicon Raman lines. *Appl. Phys. Lett*. 1982. **41**. P. 1016. https://doi.org/10.1063/1.93394.
29. Nikolenko A.S. Temperature dependence of Raman spectra of silicon nanocrystals in oxide matrix *Ukr. J. Phys*. 2013. **58**, No 10. P. 980. https://doi.org/10.15407/ujpe58.10.0980.
30. Falcao B.P., Leitao J.P., Correia M.R., Soares M.R., Wiggers H., Cantarero A., and Pereira R.N. Light-induced nonthermal population of optical phonons in nanocrystals. *Phys. Rev. B.* 2017. **95**. P. 115439. https://doi.org/10.1103/PhysRevB.95.115439.

Authors and CV

Neimash Volodymyr. Doctor of Physics. Head of radiation technology laboratory at the Institute of Physics, NAS of Ukraine. Field of research: radiation physics of condensed mater. He is the author of more than 100 science papers and technical patents.
E-mail: neimash@gmail.com

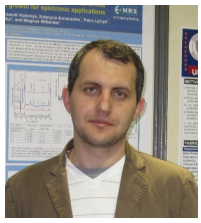

Andrii Nikolenko. Ph.D., Senior Researcher at Optical Submicron Spectroscopy Laboratory in V. Lashkaryov Institute of Semiconductor Physics, NAS of Ukraine. Field of research: semiconductor physics, semiconductor nanostructures and heterostructures, Raman, photoluminescence and FTIR spectroscopy. He is the author of more than 50 science papers and technical patents.
E-mail: nikolenko@isp.kiev.ua

Strelchuk Viktor. Professor, Doctor of Physics. Head of Optical Submicron Spectroscopy Laboratory in V. Lashkaryov Institute of Semiconductor Physics, NAS of Ukraine. Field of research: physics of semiconductors, Raman and photoluminescence spectroscopy of semiconductors, nanostructures and nanoscale materials.
He is the author of more than 100 science papers and technical patents.
E-mail: viktor.strelchuk@ccu-semicond.net

Shepeliavyi Petro. PhD in Techn. Sci., senior research scientist of the Laboratory of interference lithography at the V. Lashkaryov Institute of Semiconductor Physics, NAS of Ukraine. Field of research: inorganic resists and their application in lithography, holography, optical engineering, information recording, absorbing metal-dielectric coatings, etc. He is the author of more than 250 publications, 40 author's certificates and patents.
E-mail: spe@isp.kiev.ua

Lytvynchuk Pavlo. Leading Engineer of the Laboratory of the radiation technologies at the Institute of Physics, NAS of Ukraine. His field of scientific interests includes: semiconductor physics, radiation physics of polymers. He is the author of 2 publications.
E-mail: paulbergx@gmail.com

Melnyk Viktor. Junior research scientist of the Laboratory of radiation technologies at the Institute of Physics, National Academy of Sciences of Ukraine. His field of scientific interests includes: semiconductor physics, crystallization of amorphous silicon. He is the author of 8 science publications.

E-mail: viktor.melnyk@meta.ua

Olkhovyk Illya. Research student in laboratory of radiation technology at the Institute of Physics, National Academy of Sciences of Ukraine. His field of scientific interests includes: semiconductor physics, radiation physics of polymers. He is the author of 2 science publications.
E-mail: illia.olkhovyk@gmail.com